Chapter 6

Results: Unimodal sea state conditions

This Chapter provides the validation of the numerical procedure described in Chapter 4 for unimodal short-crested sea state conditions. The preliminary validations (Subsections 6.1.1-6.1.4) have been performed using the synthetic ship acceleration time series generated by the MATLAB code outlined in Chapter 3. Finally, Section 6.3 presents another validation based on full-scale measurements carried out on-board a containership operating in the North Atlantic.

6.1 Ship data and coordinate system

The S175 containership is employed as reference vessel in the following benchmark studies devoted to investigate the reliability of the sea state reconstruction algorithm. The choice of this ship is due to the availability of open-source data about its hydrodynamic properties (Kim et al., 2017). Table 6.1 lists the ship main dimensions.

Parameter	**Value**	**Unit**
Length between perpendiculars	175.0	m
Moulded Breadth	25.4	m
Design draught	9.5	m
Displacement	24,539	t
Pitch moment of inertia	43,286,796	tm^2
Roll moment of inertia	2,374,737	tm^2
Waterplane area	3,152	m^2
Longitudinal metacentric radius	206.0	m
Block coefficient	0.572	—

Table 6.1: Main dimensions of the S175 containership.

In the numerical simulations, a right-handed coordinate system x, y, z is assumed, as shown

in Figure 6.1, with the $x-axis$ along the longitudinal direction, $z-axis$ in the vertical direction upward positive, and passing through the center of gravity of the ship, and the $y-axis$ perpendicular to the latter one and port-side positive. The ship motions along the x, y and z axis are the *surge*, *sway* and *heave* motions, respectively. The angular motions about the x, y and $z-axis$ are the *roll*, *pitch*, and *yaw*, respectively.

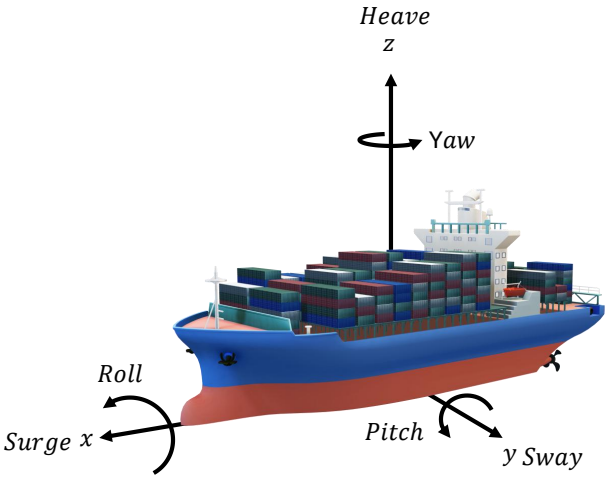

Figure 6.1: Ship axis frame.

The frequency-dependent zero-speed added massed A_{ij}^0 and radiation damping B_{ij}^0 of the S175 containership are corrected to account for the forward speed as detailed in Chapter 4. In this respect, Figure 6.2 (a)-(c) and Figure 6.3 (a)-(c) shown the added massed and the radiation dampings for heave, pitch and roll.

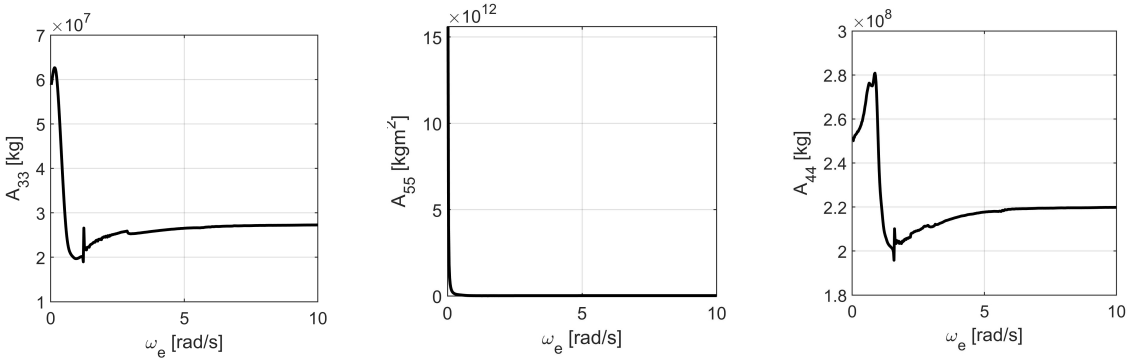

(a) Heave added mass (b) Pitch added mass (c) Roll added mass

Figure 6.2: Added mass of the S175 containership in the encounter frequency domain

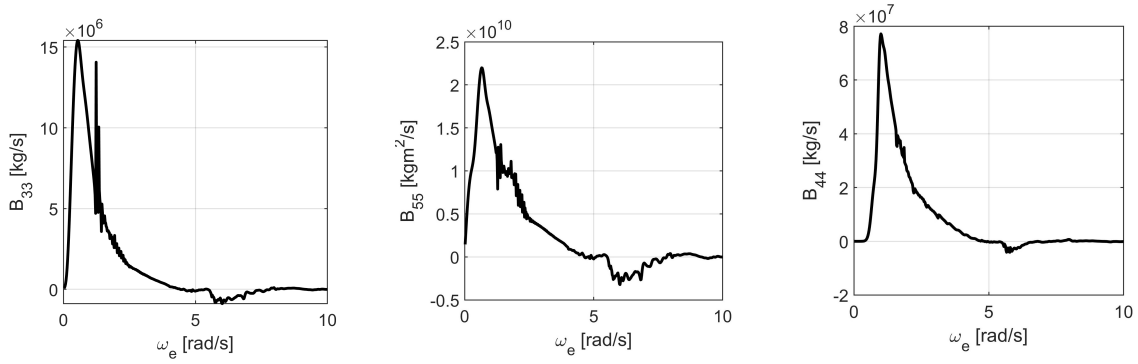

(a) Heave radiation damping (b) Pitch radiation damping (c) Roll radiation damping

Figure 6.3: Radiation damping of the S175 containership in the encounter frequency domain

Instead, the coupled heave/pitch and pitch/heave added massed and radiation damping are depicted in Figure 6.4 (a)-(d)

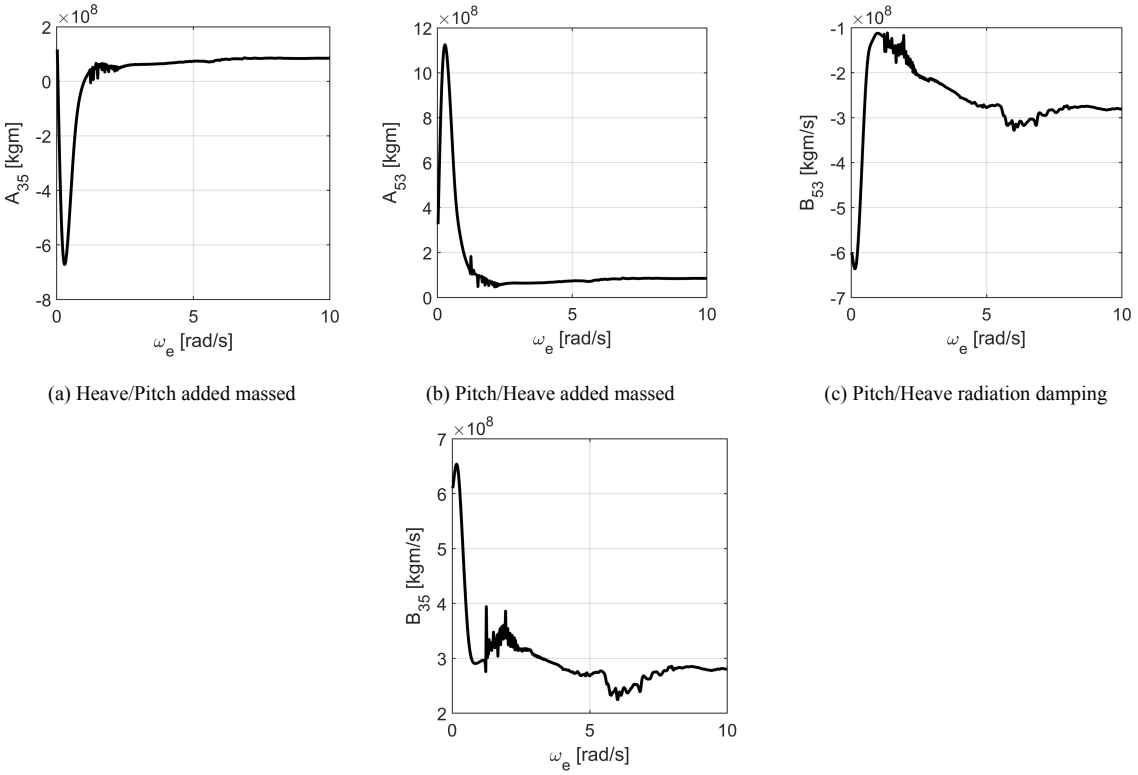

(a) Heave/Pitch added massed (b) Pitch/Heave added massed (c) Pitch/Heave radiation damping

(d) Pitch/Heave radiation damping

Figure 6.4: Coupled heave/pitch and pitch/heave added massed and radiation damping of the S175 containership

6.2 Preliminary validations of the numerical model

This section reports the benchmark study carried out in (Piscopo, 2024). The first test compares the simulated versus the estimated main wave parameters. The synthetic ship motion dataset has been determined considering all heading angles in the range between 0 and 180

deg, with a step of 30 deg steps. The significant wave height and peak period have been randomly varied between 0.5 and 5.0 m and from 6 to 20 s, respectively. Similarly, the peak enhancement factor of the JONSWAP spectrum and the spreading parameter have been systematically varied, as reported in Table 6.2. At each heading angle, 100 time series were simulated by the code described in Chapter 3, fixing the vessel speed at 20 kn and considers a same time duration equal to 1 h, with a sampling frequency of 10 Hz.

Parameter	**Range**	**Unit**
Significant wave height (H_s)	0.5–5.0	m
Wave peak period (T_p)	6–20	s
Shape parameter (γ)	1–3	adim
Spreading parameter (n)	2–4	adim
Heading angle (μ)	0–180	deg

Table 6.2: Summary of the main input parameters

Table 6.3 provides the Mean Absolute Errors between the simulated versus the estimated main wave parameters for each selected heading angle based on 100 ship motion time history with H_s, T_p and γ randomly varying in the reference interval listed in Table 6.2. The mean absolute error is computed for the significant wave height, peak wave period and the heading angle by Equations 6.1 to 6.3:

$$\mathrm{MAE}(H_s) = \frac{1}{N}\sum_{k=1}^{N}\frac{\left|H_{s,i,\mathrm{Estimated}} - H_{s,i,\mathrm{Simulated}}\right|}{H_{s,i,\mathrm{Simulated}}} \tag{6.1}$$

$$\mathrm{MAE}(T_p) = \frac{1}{N}\sum_{k=1}^{N}\frac{\left|T_{p,i,\mathrm{Estimated}} - T_{p,i,\mathrm{Simulated}}\right|}{T_{p,i,\mathrm{Simulated}}} \tag{6.2}$$

$$\mathrm{MAE}(\mu) = \frac{1}{N}\sum_{k=1}^{N}\min\{\eta_k,\ (360° - \eta_k)\} \tag{6.3}$$

with $\eta_k = \left|\mu_{i,\mathrm{Estimated}} - \mu_{i,\mathrm{Simulated}}\right|$.
The mean absolute error on the significant wave height and the wave peak period are reported in non dimensional forms, while that one relative to the heading angle is measured in degs.

Parameter	**0**	**30**	**60**	**90**	**120**	**150**	**180**
MAE H_s [adim]	0.057	0.060	0.038	0.026	0.026	0.020	0.020
MAE T_p [adim]	0.034	0.031	0.028	0.018	0.013	0.010	0.008
MAE μ [deg]	2.900	1.800	0.900	0.100	1.400	1.300	2.300

Table 6.3: Mean absolute errors of the main wave parameters at various heading angles.

By Table 6.3, it can be gathered that the minimum MAE on the significant wave height is 2%

while the maximum one occurs at 30 deg and is equal to about 6%. As concerns the wave peak period, the MAEs at head and following seas are equal to 0.8% and 3%, respectively. Finally, the maximum MAE on the hading angle is equal to 2.9 deg at following seas. To resume, it can be generally noted from Table 6.3 that the reliability of the algorithm is the maximum at beam seas, namely 90 deg, where the Doppler shift effect is null. Instead, the maximum mean absolute errors occur at the following seas due to the 3-to-1 multivalued problem between the absolute and encounter wave frequency.
A similar analysis is reported in Table 6.4, which is based on wave peak period classes, ranging from 6 to 20 secs with 2 s intervals. Table 6.4 shows that the reliability of the algorithm is almost independent of the wave period. Indeed the MAEs on the significant wave height and wave peak period range from about 2% to 4%.

Parameter	**6–8**	**8–10**	**10–12**	**12–14**	**14–16**	**16–18**	**18–20**
MAE H_s [adim]	0.040	0.021	0.042	0.043	0.032	0.037	0.036
MAE T_p [adim]	0.011	0.021	0.035	0.021	0.016	0.021	0.017
MAE μ [deg]	1.563	0.909	1.869	1.528	1.228	1.600	2.151

Table 6.4: Mean absolute errors of the wave parameters as a function of wave peak period values.

6.2.1 Performance analysis as a function of time history duration

An additional dataset was simulated and tested to investigate the incidence of the time length duration on the estimation of the sea state parameters. In this case, a set of 500 ship motion time series was simulated by the MATLAB code, randomly varying the significant wave height and the wave peak period in the range of 0.5 to 5.0 m and 6 to 20 sec, respectively and the heading angle from 0 to 360 degs. The reliability of the algorithm is test by systematically reducing the ship motion time series from 60, up to 30, 20 and 15 min as reported in Table 6.5.

Time length [s]	**60**	**30**	**20**	**15**
MAE H_s [adim]	0.030	0.056	0.069	0.083
MAE T_p [adim]	0.017	0.027	0.034	0.047
MAE μ [deg]	2.340	3.440	4.440	5.420

Table 6.5: Mean absolute errors of the wave parameters as a function of time history length.

As it can be noted, the MAEs increase among the time length reduces, as predictable. In this respect, Figure 6.5(a)–(d), provide a comparative analysis between the estimated and simulated values at different time interval. Particularly, the blue area refers to resemble of the values of the sea state parameter less than 5%, while the green (pink) area refers to relative

errors lying in the range from 5 to 10% (from 10 to 15%). Finally, the grey area refers to errors greater than 30 degs. Most of the data lie in the blue and green areas, so proving the effectiveness of the sea spectrum reconstruction procedure. As it can be noted, the reliability of the algorithm depends on the signal, as predicable.

6.2.2 Statistics of errors

Figure 6.6 (a)–(d) depict the statistics of errors on the significant wave height, the wave peak period and the heading angle. The absolute error on the significant wave height and the wave peak period follows the exponential distribution, so proving the high reliability of the sea state estimation algorithm. Instead, as concerns the heading angle it is not possible to detect the best-fit probability density function, because the bin size is too wide, as it corresponds to the heading angle bin step employed in the iterative procedure that is equal to 10 deg. Nevertheless, more information about the reliability of the assessment of the main wave parameters can be obtained, computing the errors at various quartiles, as reported in Table 6.6.

By Table 6.6 is highlighted a strong dependence of the errors on the time history length. Be-

Quantile	**Variable**	**60 min**	**30 min**	**20 min**	**15 min**
0.50	$\varepsilon[H_s]$	0.0209	0.0385	0.0480	0.0578
	$\varepsilon[T_p]$	0.0116	0.0190	0.0237	0.0328
	$\varepsilon[\mu]$	0	0	0	0
0.75	$\varepsilon[H_s]$	0.0419	0.0771	0.0960	0.1156
	$\varepsilon[T_p]$	0.0232	0.0381	0.0473	0.0657
	$\varepsilon[\mu]$	0	10	10	10
0.90	$\varepsilon[H_s]$	0.0695	0.1280	0.1595	0.1941
	$\varepsilon[T_p]$	0.0385	0.0633	0.0786	0.1091
	$\varepsilon[\mu]$	10	10	10	10
0.95	$\varepsilon[H_s]$	0.0905	0.1665	0.2075	0.2499
	$\varepsilon[T_p]$	0.0501	0.0823	0.1022	0.1419
	$\varepsilon[\mu]$	10	10	20	20
0.99	$\varepsilon[H_s]$	0.1392	0.2560	0.3189	0.3841
	$\varepsilon[T_p]$	0.0770	0.1265	0.1572	0.2181
	$\varepsilon[\mu]$	20	20	30	30

Table 6.6: Statistics of errors relative to the main wave parameters.

sides, the error relative to the wave peak period is generally about one-half of the significant wave height one, independently of the time history length. As concerns the heading angle, the error remains below 10 deg for the 0.50 quartile in all cases, although it slightly increases for higher quartiles, reaching values up to 30 deg in a correspondence of 20 and 15 min time

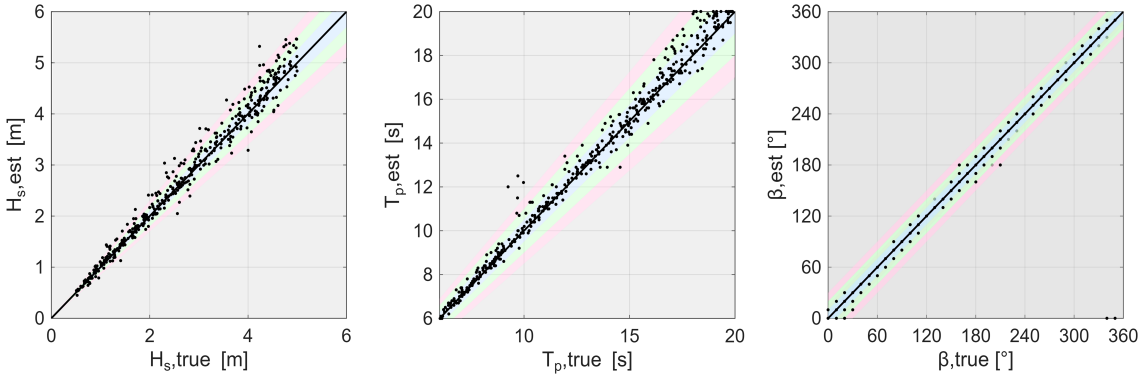

(a) Time interval = 60 min

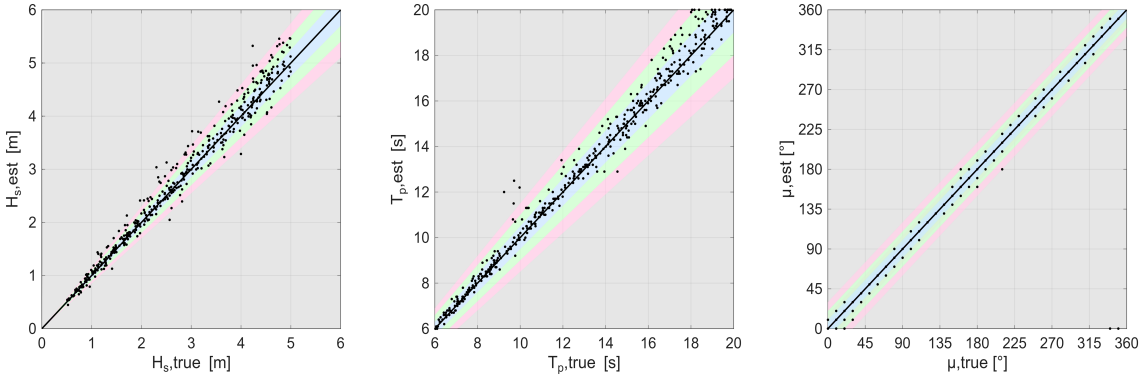

(b) Time interval=30 min

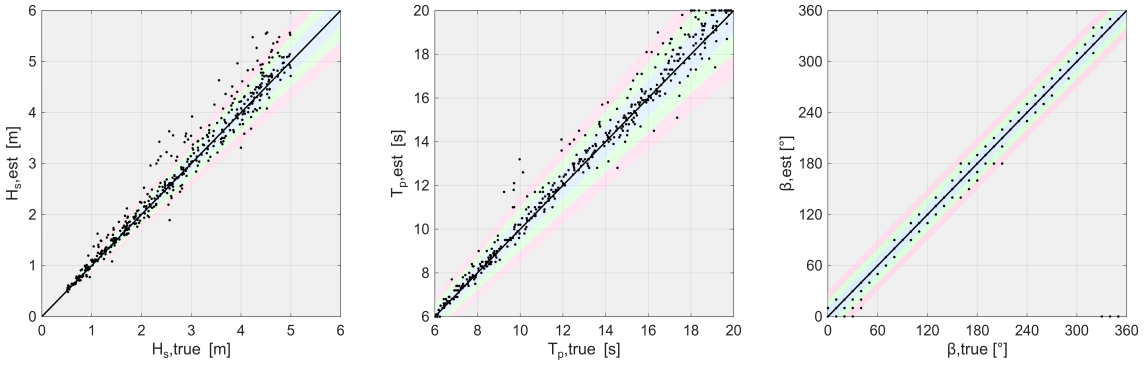

(c) Time interval=20 min

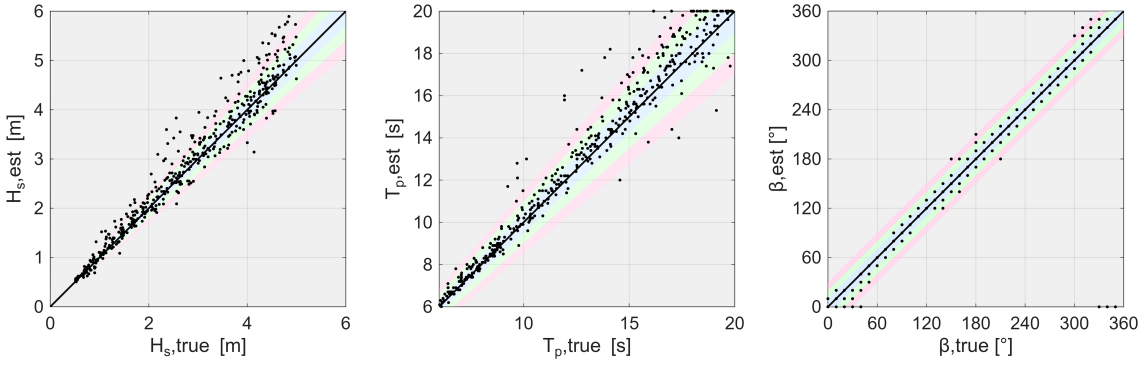

(d) Time interval=15 min

Figure 6.5: Assessment of main wave spectrum parameters as a function of time history length.

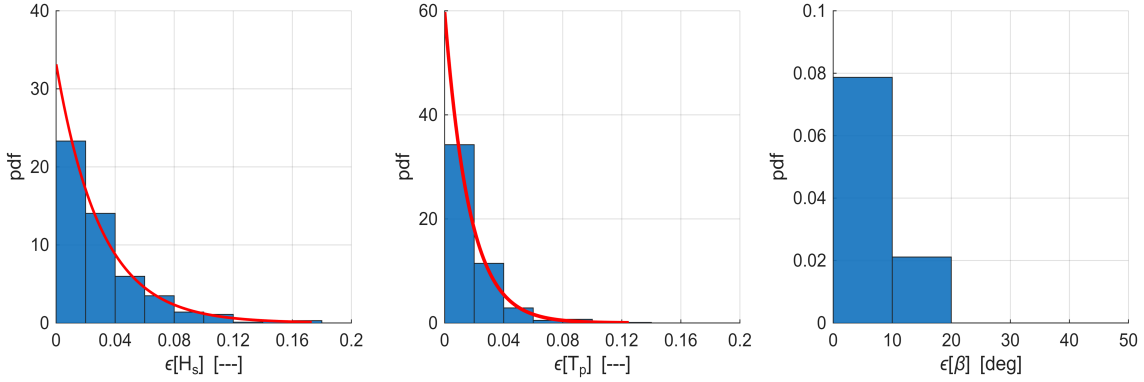

(a) Time interval = 60 min

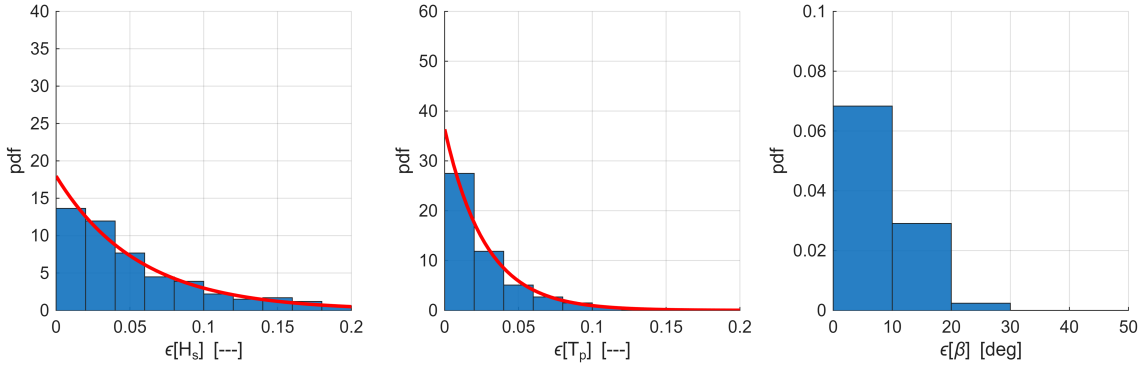

(b) Time interval=30 min

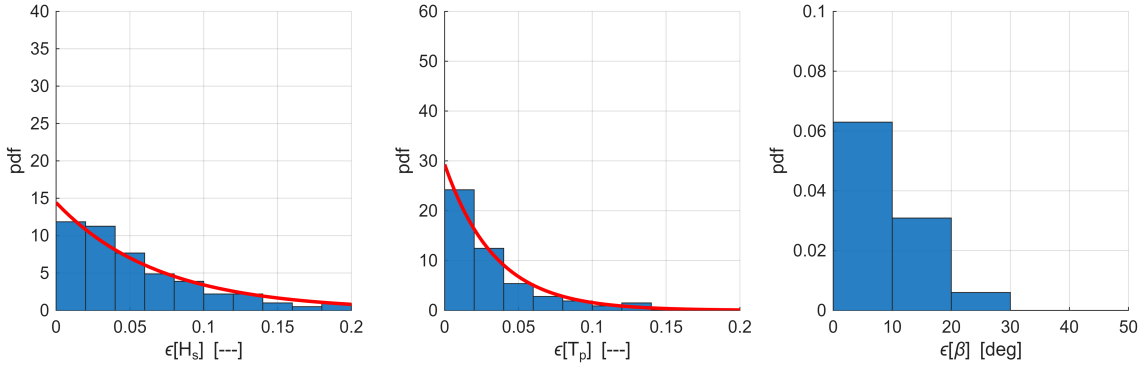

(c) Time interval=20 min

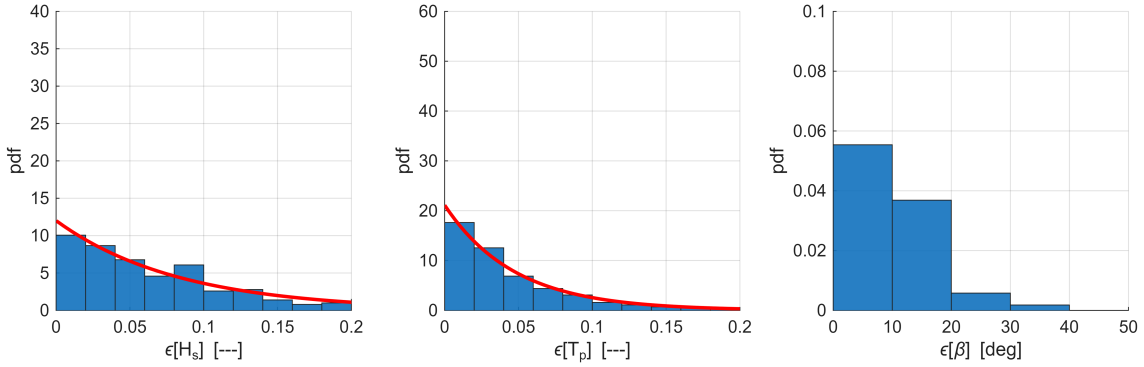

(d) Time interval=15 min

Figure 6.6: Statistics of errors as a function of time history duration.

history length. Based on these remarks, some outcomes can be stressed about the selection of the minimum time duration of ship motion signals for practical purposes:

I. The 60-minute time interval is not reliable, due to the excessively long time updating of sea state conditions;

II. The 30-minute time interval is the most suitable compromise to balance fast the updating of sea state conditions without excessively penalising the reliability of the estimated sea state parameters. In this case, the maximum errors relative to the significant wave height and wave peak period are less than about 25.0% and 12.5% in 99% of cases, according to Table 6.6. Besides, the heading angle error is less than 10 degs and 20 degs in about 70% and 98% of cases, respectively;

III. If a faster updating of sea state conditions is required, a 20-minute time interval can be considered as available option, even if a slight decrease of the reliability on the estimated sea state parameters occurs. In this case, the maximum errors, relative to the significant wave height and the wave peak period corresponding to the 99th quantile of the relevant exponential distributions, increase up to about 32% and 16%, respectively. Besides, the heading angle error is less than 10 and 30 degs in about 60% and 93% of cases;

IV. Time intervals less than 20 min should be in any case avoided, to ensure the reliability of estimated sea state parameters. Based on these considerations, it is suggested that a time interval equal to 30 min and, in any case, not less than 20 min should be selected in order to balance the reliability of the algorithm and the fast updating of sea state conditions.

6.2.3 Comparison between linear and rank correlation methods

In the following sensitive analysis on the employment of linear and rank spectral correlation methods is carried out to investigate which one guarantees the best performance for estimation the sea state parameters (Ascione et al., 2024). In this respect, three different correlation coefficients are employed and compared:

- Pearson's correlation coefficient method introduced in 1896 to measure the strength of linear relationships between two variables (Sedgwick, 2012), is defined by Equation 6.4:

$$r_p(x,y) = \frac{\sum(x_i - \overline{x})(y_i - \overline{y})}{\sqrt{\sum(x_i - \overline{x})^2} \cdot \sqrt{\sum(y_i - \overline{y})^2}} \tag{6.4}$$

  where x_i and y_i are the values of the two variables, $\overline{x}$ and $\overline{y}$ denote the mean values and n is the relevant length. The numerical value and the sign of the correlation coefficient indicate the magnitude of the correlation coefficient. Three correlation cases can be

distinguished: negative, positive, or when the correlation coefficient is close to 0, no linear correlation between the variables. A positive correlation exists when large values of one variable go along with large values of the other one or when small values of one variable go along with small values of the other variable. A negative correlation exists when large values of one variable go along with small values of the other variable and viceversa;

- The Spearman rank correlation coefficient r_s is a non-parametric rank statistical technique used to describe the relationship between two variables. It is generally used when Pearson's correlation is not applicable or misleading. Unlike Pearson's coefficient, Spearman's coefficient requires that the variables do not have to be in a linear relationship; indeed, each sample is converted into ranks before computing the correlation. Spearman's coefficient is mathematically expressed by Equation 6.5:

$$r_s(x, y) = \frac{\sum R(x_i - \overline{x})R(y_i - \overline{y})}{\sqrt{\sum (R(x_i - \overline{x})^2 R(y_i - \overline{y})^2}} \tag{6.5}$$

  where R indicates the rank of the two variables.

- Kendall's correlation τ is based on counting the number of concordant or discordant value pairs, as shown in Table 6.7. Supposing the existence of two different variables, x and y, with n_{ij} values, the number of concordant and discordant pairs is determined by the sign of the rank of the correlation between the variables for column x_a and column y_b. The Kendall Tau rank correlation coefficient τ performs even more robustly and efficiently than the Spearman one. It is defined by Equation 6.6:

$$\tau = \frac{n_c - n_d}{0.5N(N-1)} \tag{6.6}$$

  where n_c and n_d are the number of concordant and discordant pairs. As for the Pearson correlation coefficient, Kendall tau also varies in the interval from -1 $+1$.

Condition	**Description**	**Value**
$(x_{a,i} - x_{a,j})(y_{b,i} - y_{b,j}) > 0$	Concordant	$+1$
$(x_{a,i} - x_{a,j})(y_{b,i} - y_{b,j}) < 0$	Discordant	-1
$(x_{a,i} - x_{a,j})(y_{b,i} - y_{b,j}) = 0$	–	0

Table 6.7: Classification of pair comparisons based on sign agreement between differences (used in Kendall's τ coefficient).

A set of 100 time series of ship motions (simulated with the code described in Chapter 2) has been employed in the analysis: the heading angle ranges from 0 to 180 degs with a 30 deg

step, while the significant wave height and the wave peak period vary as detailed in Table 6.2. In this respect, Table 6.8 provides the mean absolute errors computed are the main wave direction, the significant wave height and the wave peak period, respectively. As can be gathered from Table 6.8, it has been verified that the rank-correlation algorithms, perform in any case better than the Pearson correlation coefficient. These results are also graphically reported in Figure 6.7, from which it is gathered that the red and orange lines (Spearman and Kendall) have a similar trend compared to the blue one (Pearson).

μ	-	**0**	**30**	**60**	**90**	**120**	**150**	**180**
MAE μ	Pearson	6.20	7.60	1.80	1.10	5.50	6.00	2.80
	Spearman	2.90	2.90	0.90	0.40	1.40	2.10	2.30
	Kendall	2.50	2.90	0.60	0.20	1.30	1.80	2.30
MAE H_s	Pearson	0.08	0.12	0.11	0.08	0.06	0.03	0.03
	Spearman	0.06	0.06	0.04	0.04	0.03	0.02	0.02
	Kendall	0.05	0.06	0.04	0.03	0.03	0.02	0.02
MAE T_p	Pearson	0.08	0.09	0.12	0.11	0.06	0.02	0.02
	Spearman	0.03	0.03	0.03	0.04	0.01	0.01	0.01
	Kendall	0.03	0.02	0.02	0.02	0.01	0.01	0.01

Table 6.8: Comparative analysis between Pearson, Spearman, and Kendall correlation coefficients

6.3 Validation using full-scale data from a containership

The numerical procedure for unimodal sea sate conductions has been further validated based on a full-scale ship motion dataset to evaluate its performance under more realistic and general scenarios. The dataset was provided thanks to the cooperation between the DTU and the Det Norske Veritas, and it consists of the full-scale ship motion measurements carried out onboard a 2,800 TEU Panamax containership. In this respect, Table 6.9 provides the ship main dimensions.